ARTICLE
Journal of Cellular Biochemistry 114:2834–2841 (2013)

Journal of Cellular Biochemistry

Hypoxia Preconditioning of Mesenchymal Stromal Cells Enhances PC3 Cell Lymphatic Metastasis Accompanied by VEGFR-3/CCR7 Activation

Xin Huang,[1] Kunkai Su,[2] Limin Zhou,[3] Guofang Shen,[3] Qi Dong,[1] Yijia Lou,[3#] and Shu Zheng*

[1]*Key Laboratory of Cancer Prevention and Intervention, China National Ministry of Education, Key Laboratory of Molecular Biology in Medical Science, 2nd Affiliated Hospital, Zhejiang University, Hangzhou 310009, China*

[2]*Bioinformation Branch, State Key Laboratory for Diagnosis and Treatment of Infectious Diseases, 1st Affiliated Hospital, Zhejiang University, Hangzhou 310003, China*

[3]*Institute of Pharmacology, Toxicology and Biochemical Pharmaceutics, Zhejiang University, Hangzhou 310058, China*

ABSTRACT

Mesenchymal stromal cells (MSCs) in bone marrow may enhance tumor metastases through the secretion of chemokines. MSCs have been reported to home toward the hypoxic tumor microenvironment in vivo. In this study, we investigated prostate cancer PC3 cell behavior under the influence of hypoxia preconditioned MSCs and explored the related mechanism of prostate cancer lymphatic metastases in mice. Transwell assays revealed that VEGF-C receptor, VEGFR-3, as well as chemokine CCL21 receptor, CC chemokine receptor 7 (CCR7), were responsible for the migration of PC3 cells toward hypoxia preconditioned MSCs. Knock-in *Ccr7* in PC3 cells also improved cell migration in vitro. Furthermore, when PC3 cells were labeled using the *hrGfp*-lentiviral vector, and were combined with hypoxia preconditioned MSCs for xenografting, it resulted in an enhancement of lymph node metastases accompanied by up-regulation of VEGFR-3 and CCR7 in primary tumors. Both PI3K/Akt/IκBα and JAK2/STAT3 signaling pathways were activated in xenografts in the presence of hypoxia-preconditioned MSCs. Unexpectedly, the p-VEGFR-2/VEGFR-2 ratio was attenuated accompanied by decreased JAK1 expression, indicating a switching-off of potential vascular signal within xenografts in the presence of hypoxia-preconditioned MSCs. Unlike results from other studies, VEGF-C maintained a stable expression in both conditions, which indicated that hypoxia preconditioning of MSCs did not influence VEGF-C secretion. Our results provide the new insights into the functional molecular events and signalings influencing prostate tumor metastases, suggesting a hopeful diagnosis and treatment in new approaches. J. Cell. Biochem. 114: 2834–2841, 2013. © 2013 Wiley Periodicals, Inc.

KEY WORDS: MESENCHYMAL STROMAL CELL; HYPOXIA PRECONDITIONING; PROSTATE CANCER; CCR7; VEGFR-3; LYMPHATIC METASTASIS

Prostate cancer is the second leading type of cancer in men in industrialized countries. Lymph node involvement denotes a poor outcome for patients with prostate cancer [Denis and Griffiths, 2000]. Prostate cancer frequently metastasizes to the bone, and the interaction between cancer cells and the bone microenvironment is crucial in the establishment of metastases. Bone marrow-derived mesenchymal stromal cells (MSCs) secrete various cytokines that regulate the behavior of neighboring cells [Cooper et al., 2003]. The chemotactic responses to bone-derived factors and the interaction of prostate cancer cells with the bone microenvironment are of paramount importance [Cooper et al., 2003]. MSCs are pivotal for neuroblastoma metastasis via the secretion of stromal cell-derived factor-1 [Ma et al., 2011]. MSCs within tumor stroma promote breast cancer metastasis [Karnoub et al., 2007].

Grant sponsor: Zhejiang Governmental Principle International Cooperation; Grant number: 2009C14010; Grant sponsor: Young Researcher Foundation of Health Bureau in Zhejiang Province; Grant number: 2011RCA024.

*Correspondence to: Shu Zheng, MD, PhD, Key Laboratory of Cancer Prevention and Intervention, China National Ministry of Education, Key Laboratory of Molecular Biology in Medical Science, 2nd Affiliated Hospital, Zhejiang University, Hangzhou 310009, China. E-mail: zhengshu@zju.edu.cn

#Correspondence to: Yijia Lou, PhD, Institute of Pharmacology, Toxicology and Biochemical Pharmaceutics, Zhejiang University, Hangzhou 310058, China. E-mail: yijialou@zju.edu.cn

Manuscript Received: 19 May 2013; Manuscript Accepted: 24 July 2013

Accepted manuscript online in Wiley Online Library (wileyonlinelibrary.com): 12 August 2013

DOI 10.1002/jcb.24629 • © 2013 Wiley Periodicals, Inc.

However, little is known regarding the role of MSCs in lymphatic prostate cancer metastases.

Solid tumors develop hypoxia due to inadequate O_2 supply. Hypoxia is a key inducer triggering vascular endothelial growth factor (VEGF) expression via the hypoxia-inducible factor 1α (HIF1α) transcription complex, which is essential for tumor growth, invasion and metastasis [Li et al., 2004; Zhong et al., 2004]. VEGF receptor (VEGFR) 2 and 3 are essential for the functions of vascular endothelium and lymphatic endothelium, respectively [Olsson et al., 2006]. One hypothesis postulates that VEGF-C-induced tumor lymphangiogenesis is the primary mechanism underlying VEGF-C-enhanced lymphatic metastasis [Mandriota et al., 2001; Veikkola et al., 2001]. Based on our knowledge, little is known regarding the role of MSCs within tumor stroma promoting cancer cell metastasis deals with the influence of hypoxia.

Recently, MSCs have been reported to home towards the hypoxic tumor microenvironment in vivo, and hypoxic tumor cells specifically recruit MSCs through the activation of survival pathways that facilitate tumor progression [Rattigan et al., 2010]. However, hypoxia seems not always promoting tumor progression. β2-Adrenergic receptor signaling does not appear to be a facilitator of cancer expansion under hypoxic conditions in vitro. This suggests that the effects are dependent on tissue type and on the degree and duration of hypoxia [Baloğlu et al., 2009], highlighting the need to manage the degree and duration of hypoxic conditions in vitro. Another example reported as follows, the sensitivity of osteosarcoma cells is significantly decreased under hypoxia, while that of MSCs is not. Furthermore, HIF-1α expression is unchanged in osteosarcoma cells and increased in MSCs [Kido et al., 2012], suggesting that MSCs play major roles in certain tumors under hypoxia. Therefore, we employ hypoxia-preconditioned MSCs (H-MSCs) to explore prostate cancer behaviors under the influence of hypoxia, and the insights have shed light onto the need of the stable degree and duration of hypoxic conditions.

Chemokines are grouped into four families (C, CC, CXC, and CX3C) according to their ligands. The biological activities are mediated by their interaction with the chemokine receptor family of G-protein-coupled receptors [Murphy et al., 2000]. CC chemokine receptor 7 (CCR7) is expressed on all naive T-cells, some memory T-cells, B-cells, and mature dendritic cells [Baggiolini, 1998]. CCR7 interacts with its ligands, chemokine ligand 19 (CCL19) and 21 (CCL21) [Zlotnik and Yoshie, 2000], and plays important roles in lymphocyte trafficking and homing to lymph nodes during immune and inflammatory reactions [Dieu et al., 1998; Sozzani et al., 1998; Hirao et al., 2000]. Crosstalk of tumor cell with lymphatic tissue via VEGF-C and CCR7 messages promotes invasion [Issa et al., 2009; Chaudary and Hill, 2011]. Although CCR7 is expressed in the malignant tissue of prostate cancer patients [Heresi et al., 2005], whether the CCL21-CCR7 axis enables prostate cancer lymphatic invasion and metastasis under the influence of H-MSCs has not been reported yet.

To date, it remains unclear whether H-MSCs, which mimic the MSCs in a hypoxic tumor microenvironment, can enhance prostate cancer metastases. In the current study, we employ H-MSCs to explore prostate cancer cell behaviors under the influence of hypoxia in vitro. Meanwhile, we apply an H-MSC/PC3 as a novel stromal cancer cell interaction xenograft model to mimic the hypoxic tumor microenvironment in vivo. We aim to evaluate whether H-MSCs undertake major roles in the malignant behavior of prostate cancer by focusing primarily on VEGFRs and the CCL21/CCR7 axis. Therefore, the data observed here can aid in the understanding of the underlying mechanisms of H-MSC-modulated metastasis in prostate cancer and facilitate the design and development of therapeutic approaches.

MATERIALS AND METHODS

CELL CULTURE

Human MSCs were harvested from the bone marrow of four healthy donors (Donor #13, #16, #21 and #22) with written consent from the Ethics Committee of the Zhejiang University and the 2nd Affiliated Hospital at the Zhejiang University School of Medicine. Adherent cells were isolated and cultured in L-DMEM (GIBCO, Grand Island) with 20% fetal bovine serum (GIBCO), penicillin (100 U/ml), and streptomycin (100 μg/ml) in 5% CO_2 at 37°C. Recombinant human CCL21 (rhCCL21) was obtained from R&D (Minneapolis) and used at a final concentration of 10 ng/ml. The cancer cell lines CEM, CWR22Rv1, LNCaP, PC3 and DU145 were purchased from the Type Culture Collection of the Chinese Academy of Sciences (Shanghai, China) and cultured in RPMI1640 (HyClone, UT) with 5% FBS (GIBCO) in the conditions listed above.

LENTIVIRUS INFECTION

The *hrGfp*-lentivirus used in this study was a generous gift from Dr. Duanqin Pei at the Guangdong Health Research Institute, China. The human CCR7 gene was cloned from CEM cells and ligated into the CMV-IRES-eGFP backbone for lentiviral vector packaging. Both lentiviral vectors were used to transduce human prostate cancer cells at MOI = 10 for 24 h. Infection efficiency was tested 48 h after medium replacement.

HYPOXIA PRECONDITIONING AND CONDITIONED MEDIUM

Human MSCs were cultured under normoxic (20% O_2) or hypoxic conditions (0.5% O_2) overnight before transplantation or in vitro experiments. At the end of preconditioning, supernatants were harvested and centrifuged at 4,000 rpm to discard cell debris. The conditioned medium (CM) was stored at −20°C.

REAL TIME QRT-PCR

Total RNA was extracted from each cell line or tissue sample using TRIzol (Invitrogen). cDNA was synthesized from 1 μg samples with the TaKaRa PrimeScript II 1st Strand cDNA Synthesis Kit (TaKaRa Bio, Inc., Shiga, Japan). A Smart Cycler II System (TaKaRa) and SYBR Premix Ex Taq (TaKaRa) were used for quantitative real time RT-PCR analysis according to the manufacturer's protocol. The index gene data was normalized to human β-actin.

TRANSWELL ASSAYS

Cells (1×10^4) were suspended in 100 μl RPMI1640 and seeded in the upper well of a transwell chamber (Corning Costar 3422 Transwell, 8.0 μm pore, Cambridge, MA). The lower well contained 600 μl of index medium. After a 48-h incubation, cells migrated into the lower well and were subsequently stained by Hoechst 33258 (Beyotime, Jiangsu, China) and counted.

FLOW CYTOMETRY

Approximately 1×10^6 cells were trypsinized and resuspended in 50 μl PBS containing fluorochrome-conjugated surface marker antibodies (Becton Dickson). Mouse monoclonal isotype antibodies were used to detect any non-specific fluorescence. After incubation in the dark for 30 min at 4°C, cells were resuspended in 500 μl PBS. Cell fluorescence was evaluated using a FACSCanto™ II instrument (BD Biosciences), and data were analyzed using CellQuest software (BD Biosciences).

XENOGRAFTS

PC3 cells (1×10^6) were combined with 1×10^6 MSCs, and subcutaneously injected into the backs of male SCID/NOD mice. The tumor volumes were measured regularly. After 9 weeks, all mice were euthanized and examined. Mouse experiments were performed according to guidelines from the animal ethics committee of Zhejiang University.

HISTOLOGY AND MICROSCOPY

Immediately after the excision of primary tumors and tissue, small pieces of tissue were fixed in 4% paraformaldehyde overnight at 4°C in paraffin-embedded blocks. All resected tissues were histologically examined by hematoxylin and eosin (H&E) staining. Fluorescent signals were observed microscopically.

WESTERN BLOT ANALYSIS

Total protein was extracted using RIPA buffer (containing 0.2% Triton X-100, 5 mmol/L EDTA, 1 mmol/L PMSF, 10 mg/ml leupeptin, 10 mg/ml aprotinin, added with 100 mmol/L NaF, and 2 mmol/L Na_3VO_4) and mixed with 15 μl Laemmli sample buffer and 1.5 μl β-mercaptoethanol before separation by SDS-PAGE. Samples were subsequently transferred to PVDF membrane filters. The transferred samples were probed with primary antibody (1:1,000) overnight at 4°C. Chemiluminescent signals were generated by incubation with the ECL reagent (Beyotime). As primary antibodies, anti-CCL21 or anti-CCR7 or anti-VEGFR-2 or anti-pVEGFR-2 or anti-VEGFR-3 or anti-β-actin was purchased from Santa Cruz Biotechnology, Inc.; anti-pJAK1 or anti-JAK1 or anti-pJAK2 or anti-JAK2 or anti-pSTAT3 or anti-STAT3 or anti-pIκBα or anti-IκBα or anti-NFκB (p50) or anti-pAkt (Thr308/Ser473) or anti-Akt or anti-pPI3K

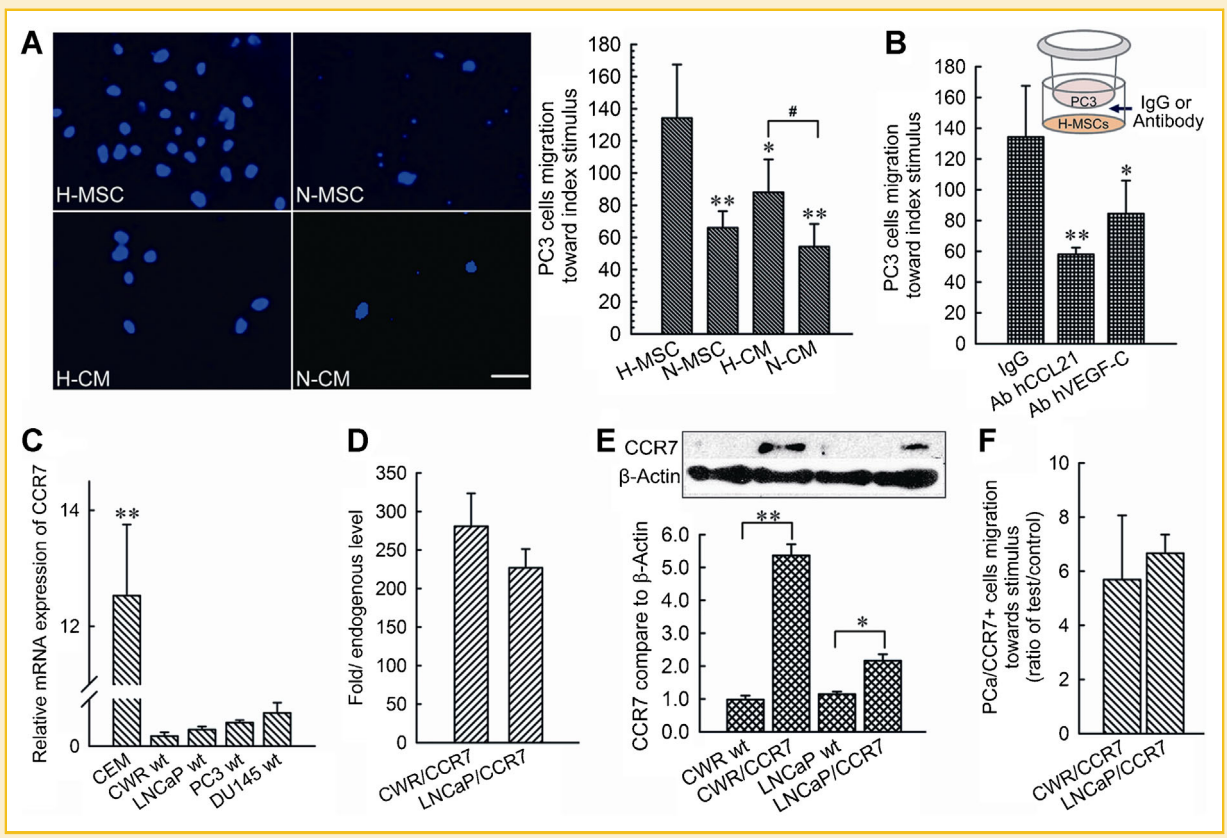

Fig. 1. Influence of hypoxia-preconditioned MSCs on prostate cancer cell migratory capacity in vitro. A: Transwell assays revealed that PC3 cells had an increased migratory capacity in the presence of H-MSCs compared to that in the presence of N-MSCs. Fluorescent images display migrated PC3 cells stained with Hoechst 33258 (blue). Cells migrated to CM served as a parallel control. B: PC3 cell migration was blocked by the addition of Ab hCCL21 or Ab hVEGF within H-CM by Transwell assays. C: Real time qRT-PCR amplification of basal *hCcr7* expression in prostate cancer cell lines and CEM cells. D: CWR and LNCaP cells were transduced with a CMV-*hCcr7*-IRES-eGFP expression vector, and the fold change of *hCcr7* was determined by real time qRT-PCR in CWR/CCR7 and LNCaP/CCR7 cells. E: Representative hCCR7 protein bands showed the expression in CWR/CCR7 and LNCaP/CCR7 cells. F: Transwell assays revealed a six- to sevenfold increase of CWR/CCR7 and LNCaP/CCR7 cells induced by rhCCL21 over control vector-transduced cells ($^{*,\#}P < 0.05$, $^{**}P < 0.01$). The data presented are mean ± SD from at least three separate experiments. Transwell assays were performed in three independent replicates. Total cells in five random fields of each membrane were counted at 400× magnification under a fluorescent microscope, Bar = 25 μm.

(p85) or anti-PI3K (p85) was purchased from Cell Signaling Technology, Inc.

STATISTICAL ANALYSIS

All experiments were carried out at least three times. For Transwell assays, each test was performed in triplicate. All values presented are the mean ± SD. Statistical significance was determined by Student's *t*-test.

RESULTS

INFLUENCE OF H-MSCS ON PROSTATE CANCER CELL MIGRATORY CAPACITY IN VITRO

Transwell assays were performed to explore prostate cancer cell migration in the presence of H-MSCs. The results revealed that PC3 cells showed an increase in their migratory capacity upon H-MSC co-culture compared to those in the presence of normoxia preconditioned-MSCs (N-MSCs). As a parallel control, PC3 cells were allowed to migrate to conditioned medium (CM). The number of migrated PC3 cells was dramatically enhanced under the presence of H-MSCs or concomitant H-CM (Fig. 1A). As expected, the migration of PC3 cells was unaffected by IgG-MSC-CM treatments, although the migration could be blocked by synergistic treatments of H-MSCs plus either an hCCL21 or hVEGF antibody (Fig. 1B). These results suggest that CCR7 and VEGFR-3 were responsible for the migration of PC3 cells towards H-MSCs.

CCL21/CCR7 AXIS ARE REQUIRED IN PROSTATE CANCER CELL MIGRATION

To confirm whether the CCL21/CCR7 axis was required for prostate cancer cell migration, the basal *Ccr7* transcription levels were

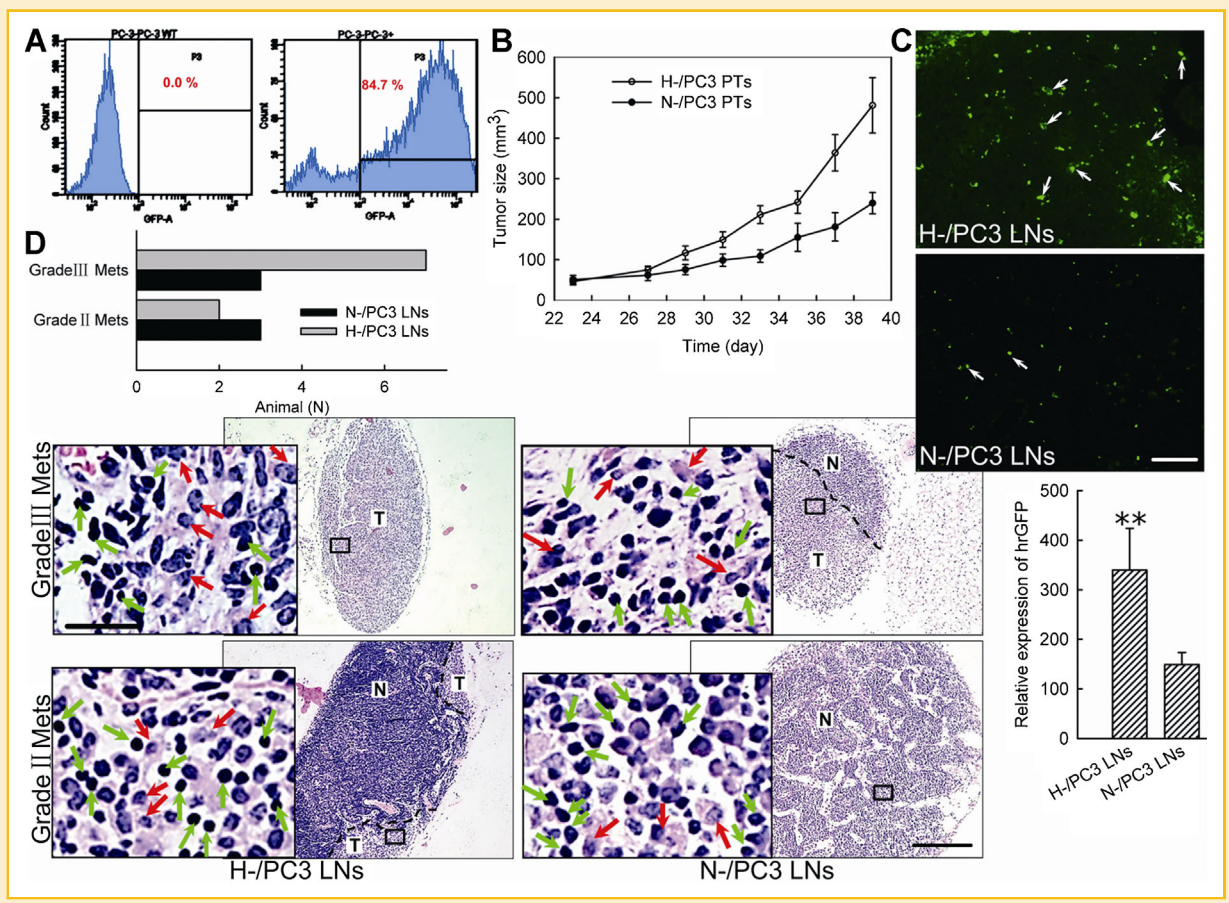

Fig. 2. H-MSCs presence leads to regional lymph node metastases of PC3 cells. A: Flow cytometry determination of the percentage of GFP positive cells. The percentage of hrGFP$^+$ PC3 cells reached 84.7%. B: Growth curve of H-/PC3 and N-/PC3 xenografts. Xenografts were generated as described in Materials and Methods Section. PTs of two groups displayed equivalent size ($P = 0.143$, N = 10, mean ± SEM). C: The hrGFP$^+$ cell expression densities were quantified. The distribution of PC3 cells in LN sections was much denser (white arrow) in mice bearing H-/PC3. Relative expression of hrGFP$^+$ in LNs were quantified for both groups ($^{**}P = 0.0019$, mean ± SD). D: H&E staining of axillary and brachial LNs. Normal lymphocytes region (N) and cancer cell invaded region (T) are distinguished. Green arrows indicate smaller and condensed lymphocyte nucleus with less cytoplasm, while red arrows represent larger and loosened cancer cell nucleus with abundant pink cytoplasmic components. Mets are graded as II and III according to the cancer cell relative invaded region in regional lymph nodes. The frequency of LN mets was quantified. Seven of ten and three of ten mice bearing grade III mets was determined in H-/PC3 and N-/PC3 group, respectively; while 2/10 and 3/10 grade II mets bearing hosts were found in respective group. PTs, primary tumors; LNs, lymph nodes; mets, metastases; N-/PC3, N-MSCs present; H-/PC3, H-MSCs present. Bars, 100 μm; bars in insets, 12.5 μm.

measured in several prostate cancer cell lines. The results revealed that expression was markedly lower in these cell lines when compared with that of CEM (Fig. 1C). Due to the less aggressiveness and relatively low level of *hCcr7*, CWR, and LNCaP cells were transduced with the CMV-*hCcr7*-IRES-eGFP vector. Both gene and protein expressions of hCCR7 were markedly up-regulated in CWR/CCR7 and LNCaP/CCR7 cells (Fig. 1D,E). The migration efficiency in response to rhCCL21 was tested using Transwell assays for both $CCR7^+$ cells. The migrated cell numbers were considerably increased over control vector-transduced cells in both $CCR7^+$ cells, reaching six- to sevenfold (Fig. 1F). This result suggested that rhCCL21 directly mediated the migration of CWR/CCR7 and LNCaP/CCR7 cells and created a favorable microenvironment for these malignant cells.

H-MSCS ENHANCE PROSTATE CANCER LYMPH NODE METASTASES

To investigate the effects of H-MSCs on prostate cancer lymph node metastases, PC3 cells were transduced with *hrGfp*-lentivirus. Flow cytometry confirmed that the percentage of $hrGFP^+$ cells reached 84.7% (Fig. 2A). The preparation and injection of H-MSC and N-MSCs combinations (H-/PC3 and N-/PC3, respectively) are described in Materials and Methods Section. As shown in Figure 2B, the growth of H-/PC3 and N-/PC3 primary tumors after injection was not significantly different. The $hrGFP^+$ cell expression densities were quantified in axillary and brachial lymph node sections for both groups. The distribution of PC3 cells in lymph nodes was much denser in mice bearing H-/PC3 (Fig. 2C). The normal lymphocyte region (N) and cancer cell-invaded region (T) were distinguished by H&E stained lymph node sections. Metastases were graded as either II or III. The frequency of grade III lymph node metastases was much higher in H-/PC3 xenograft hosts than in N-/PC3 (Fig. 2D). Seven H-/PC3 hosts had grade III mets (7/10), while three N-/PC3 hosts exhibited grade III mets (3/10). However, the frequency of hosts bearing grade II mets were similar (2/10 and 3/10, respectively).

INFLUENCES OF H-MSCS ON VEGFRS OR CCR7 EXPRESSION IN XENOGRAFTS

We tested whether the secretion of VEGF-C, as well as the expression of its cognate receptors VEGFR-2 and -3, was enhanced. Western blotting demonstrated that the expression of VEGFR-2 and -3 were affected in different manners. Both VEGFR-2 and the p-VEGFR-2/VEGFR-2 ratio were decreased, while VEGFR-3 was significantly up-regulated in H-/PC3 PTs (Fig. 3). These data suggest a selective switching-on of VEGFR-3 and switching-off of VEGFR-2 signaling in H-/PC3 PTs, given that they are expressed by lymphatic endothelial cells and angiogenic tumor blood vessels, respectively. Unlike results from other studies, VEGF-C maintained a relatively stable expression

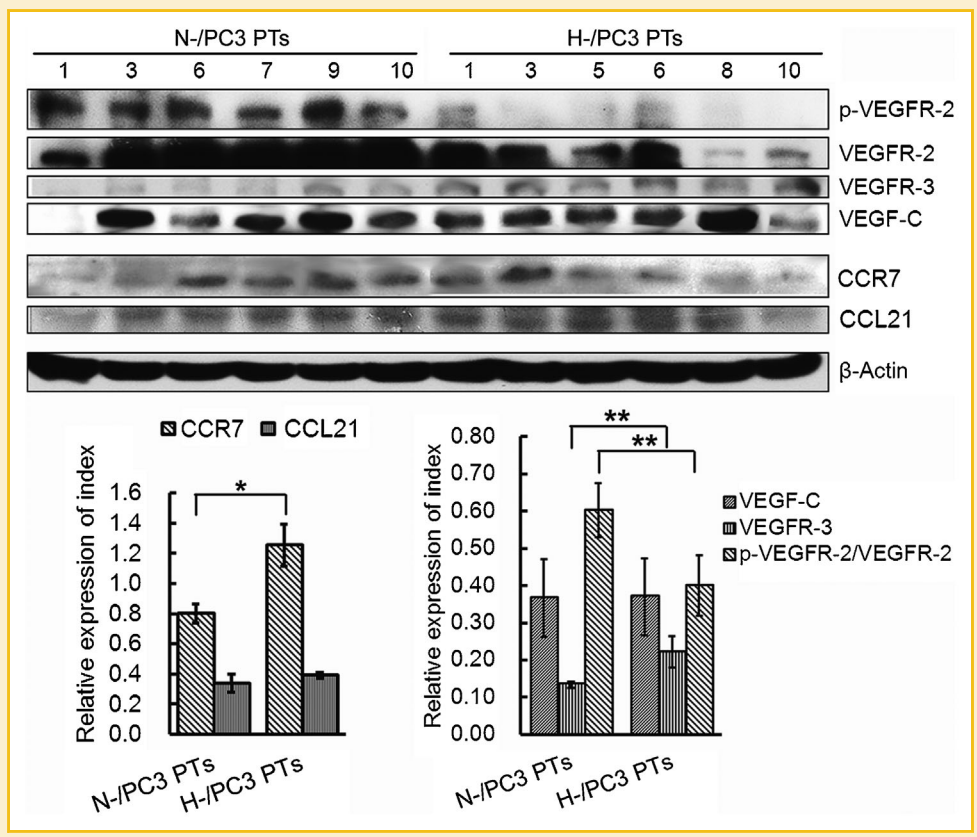

Fig. 3. Influence of H-MSCs on VEGF-C/VEGFRs or CCL21/CCR7 expression in prostate cancer xenografts. Tumor extracts were prepared followed by blotting for VEGF-C/VEGFRs or CCL21/CCR7. The relative expressions of VEGF receptor 2 and 3 as well as CCL21/CCR7 expression in H-/PC3 or N-/PC3 primary tumors (PTs) were determined by densitometry. Both VEGFR-2 and the p-VEGFR-2/VEGFR-2 ratio were decreased in H-/PC3 PTs, while VEGFR-3 was significantly up-regulated in H-/PC3 PTs; VEGF-C retained a stable expression in both conditions. CCR7 expression was upregulated in H-/PC3 PTs ($^*P < 0.05$, $^{**}P < 0.01$). Data shown are representative of at least three independent replicates. Error bars represent standard deviation.

in both conditions, which indicated that hypoxia preconditioning of MSCs did not influence VEGF-C secretion (Fig. 3). Western blotting also revealed that CCR7 expression was enhanced in H-/PC3 PTs (Fig. 3). As expected, rhCCL21 induced the elevation of the p-Akt/Akt and p-IκBα/IκBα ratios in CWR/CCR7 cells (Supplementary Fig. S1), which further supported the hypothesis that p-Akt/p-IκBα signaling was involved in prostate cancer cell chemotaxis.

FUNCTIONAL DOWNSTREAM SIGNALING PATHWAYS OF VEGFR-3 AND CCR7 IN XENOGRAFTS

We investigated the molecular events that contribute to the functional signaling pathways downstream of VEGFR-3 and CCR7. We hypothesized that NFκB was a nuclear target via a PI3K/Akt cascade in the CCL21-induced prostate cancer lymph node metastases in H-/PC3 PTs. The p-Akt (Ser473)/pAkt ratio was markedly increased in H-/PC3 PTs compared with that in N-/PC3 PTs, although the p-PI3K/PI3K and p-Akt (Thr308)/Akt ratios were only slightly increased (Fig. 4A). The p-IκBα/IκBα ratio was significantly increased in H-/PC3 PTs (Fig. 4B), which was accompanied by significantly increased p-JAK2/JAK2 and p-STAT3/STAT3 ratios and a decreased p-JAK1/JAK1 ratio (Fig. 4C). Moreover, the elevated level of phosphorylated IκBα suggests the constitutive release of NFκB. These results indicate that CCL21-induced phosphorylation of IκBα through PI3K/Akt accompanied by the selective up-regulation of p-JAK2/p-STAT3 expression have a critical role in prostate cancer cell progression and lymph node metastasis.

DISCUSSION

Researchers have proposed that bone marrow MSCs enhance tumorigenesis and metastasis in multiple ways [Kuhn and Tuan, 2010]. Hypoxia is a constant and universal feature throughout

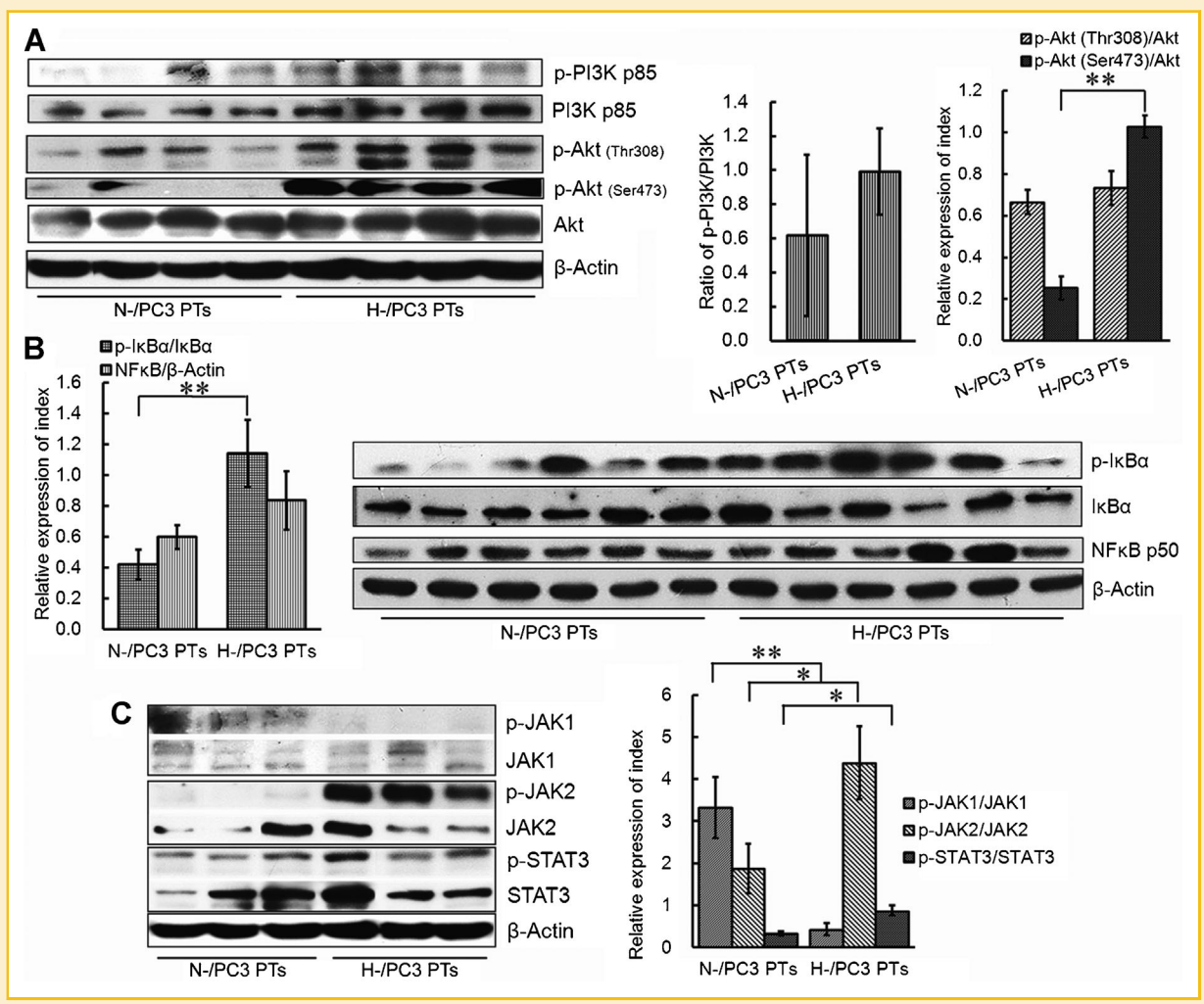

Fig. 4. Functional downstream signaling pathways involved in VEGFR-3 and CCR7 expression in PTs. Cellular extracts were prepared and blotted for phosphorylated PI3K, total PI3K, phosphorylated Akt (Thr 308 and Ser 473), total Akt, phosphorylated JAK1/2, total JAK, phosphorylated STAT3, and total STAT3. The relative expression ratios of p-PI3K/PI3K, p-Akt/Akt, p-JAK/JAK, and p-STAT3/STAT3 were determined by densitometry. A: In PTs in the presence of hypoxia-MSCs (H-/PC3), the p-PI3K/PI3K and p-Akt (Thr308)/p-Akt ratios were only slightly increased, while the p-Akt (Ser473)/pAkt ratio was markedly increased compared to that in N-/PC3 PTs. B: The p-IκBα/IκBα ratio was significantly increased in H-/PC3 PTs. C: In H-/PC3 PTs, the p-JAK2/JAK2 and p-STAT3/STAT3 ratios were significantly increased, while the p-JAK1/JAK1 ratio was decreased; $^{*}P < 0.05$, $^{**}P < 0.01$. Data shown are representative of at least three independent replicates. Error bars indicate the standard deviation.

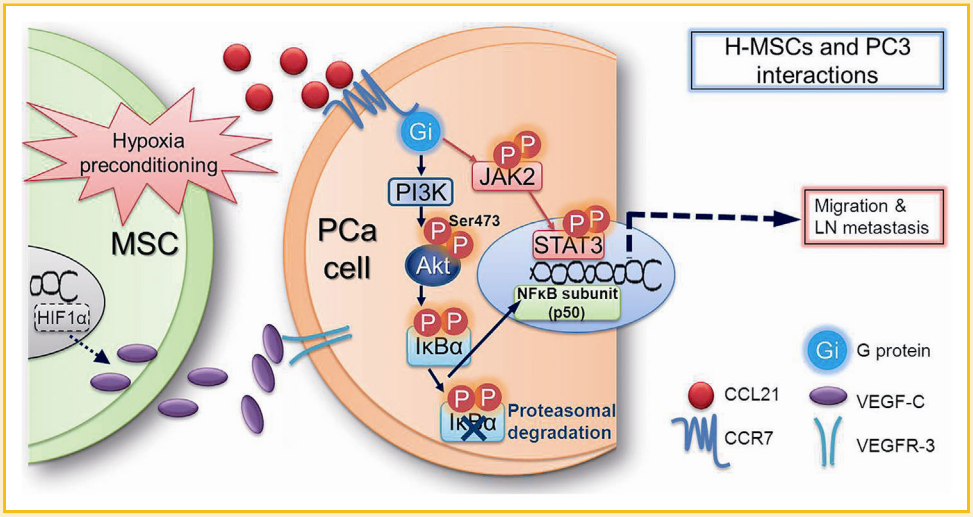

Fig. 5. The schematic diagram with the proposed mechanisms. Schematic diagram with proposed mechanisms by which H-MSCs contribute to human prostate cancer cell lymphatic metastasis via selective up-regulation of prostate cancer VEGFR-3/CCR7 expression accompanied by PI3K/Akt/IκBα and JAK2/STAT3 signaling activation. The cartoon compiles the results and conclusions of this report.

tumor progression [Rattigan et al., 2010]. The present study hypothesized that the presence of H-MSCs acted as an inducer that mimics the effect of neighboring cells under hypoxic conditions in prostate cancer. In current study, we explored the influence of H-MSCs on prostate cancer lymphatic metastases and its underlying mechanisms in a xenograft model as well as in vitro (Fig. 5).

We found that the PC3 cells were much denser in lymph nodes in H-/PC3 mice. The results from Transwell assay were consistent with that in vivo test. These results indicated that H-MSCs created a favorable microenvironment that facilitated malignant cell mobilization, while both CCR7 and VEGFR-3 were responsible for prostate cancer cells migrating towards H-MSCs. Thus, our data propose a novel research model.

Hypoxia and the consequent angiogenesis may play a major role in prostate cancer progression, given that VEGF and HIF1α are increased in prostate cancer. VEGFR-2 and VEGFR-3 are essential for angiogenesis and lymphangiogenesis. VEGF, the downstream product of HIF1α, was decreased in the HIF1α knockdown PC3 clones. In our study, we found that the presence of H-MSCs enhanced prostate cancer lymph node metastases and the selective up-regulation of VEGFR-3 and CCR7 in vivo. VEGFR-2 phosphorylation is the crucial step that initiates downstream signaling pathways leading to angiogenesis [Sinha et al., 2009]. H-/PC3 PTs exhibited a decreased p-VEGFR-2/VEGFR-2 ratio, indicating the possible switching-off of vascular signaling. Our findings indicate that VEGFR-3 was selectively activated in H-/PC3 PTs. Future work may include the knockdown of *Vegfr-3* to confirm its function in these circumstances.

Previous studies report the pro-metastatic functions of CCR7 and VEGF-C in tumors and the promotion of tumor invasion by VEGF-C toward lymphatics by both autocrine and CCR7-dependent paracrine signaling [Issa et al., 2009]. Although as well known that tumor-secreted VEGF-C was correlated with incidence of lymph node metastasis [Mandriota et al., 2001; Hirakawa et al., 2007], current study demonstrated that VEGF-C maintained a relative stable expression in H-MSCs appearance, which indicated that hypoxia preconditioning of MSCs did not influence VEGF-C secretion in vivo. This interesting finding reveals that only VEGFR expression is regulated under the influence of H-MSCs. It might be valuable in drug discovery possessing selective blocking the activated VEGFR for inhibiting tumor metastasis to distant sites.

MSCs directly promote tumor progression via cell–cell interaction, secretion of cytokines and growth factors, and the organization of an extracellular matrix [Kuhn and Tuan, 2010]. CCR7 and CCL21 have multiple biological functions [Liu et al., 2010]. In this study, enhanced migration of CWR/CCR7 and LNCaP/CCR7 cells by rhCCL21 suggested that CCL21 directly mediated the migration of CCR7-overexpressing prostate cancer cells. Furthermore, CCR7 activates the mammalian target of rapamycin (mTOR) signal by PI3K/Akt. The PI3K/Akt signaling pathway influences many other downstream molecules, including those of the NFκB family, which are tightly controlled by the IκB inhibitory family [Liu et al., 2010]. We found that NFκB p50 was released upon IκBα degradation in H-/PC3 PTs, which might contribute to the regulation of prostate cancer lymphatic metastasis.

The present study revealed a selective up-regulation of p-JAK2/p-STAT3 expression and down-regulation of p-JAK1 expression in H-/PC3 PTs. JAKs and STATs, especially STAT3, are constitutively activated in human cancers and induce target gene expression. The JAK1/STAT3 signaling pathway regulates VEGF expression in the occurrence and progression of human meningioma [Park et al., 2013]. In the current xenograft model, the down-regulation of VEGFR-2/p-JAK1 might aid in better understanding the selective VEGFR-3/p-JAK2 signaling, which promotes lymphatic-specific metastases in prostate cancer.

Taken together, our data indicate that H-MSCs enhance prostate cancer lymphatic metastases selectively via VEGFR-3 and CCR7 signaling without influence in VEGF-C expression. Our findings may facilitate the understanding of the mechanisms that regulate

H-MSCs-modulated metastasis in prostate cancer, leading to the design and development of specific therapeutic approaches.

ACKNOWLEDGMENTS

We sincerely acknowledge the technical assistance by Ms. Yan Liu in the Stem Cell Lab at the Institute of Pharmacology, Toxicology and Biochemical Pharmaceutics. This study was supported by the Zhejiang Governmental Principle International Cooperation Projects (No. 2009C14010 to Zheng) and Young Researcher Foundation of Health Bureau in Zhejiang Province (No. 2011RCA024 to Huang).

REFERENCES

Baggiolini M. 1998. Chemokines and leukocyte traffic. Nature 392:565–568.

Baloğlu E, Ke A, Abu-Taha I, Bärtsch P, Mairbäurl H. 2009. In vitro hypoxia impairs β2-adrenergic receptor signaling in primary rat alveolar epithelial cells. Am J Physiol Lung Cell Mol Physiol 296:L500–L509.

Chaudary N MM, Hill RP. 2011. Suppression of vascular endothelial growth factor receptor 3 (VEGFR3) and vascular endothelial growth factor C (VEGFC) inhibits hypoxia-induced lymph node metastases in cervix cancer. Gynecol Oncol 123:393–400.

Cooper C, Chay C, Gendernalik J, Lee H, Bhatia J, Taichman R, McCauley L, Keller E, Pienta K. 2003. Stromal factors involved in prostate carcinoma metastasis to bone. Cancer 97(3Suppl):739–747.

Denis L, Griffiths K. 2000. Endocrine treatment in prostate cancer. Semin Surg Oncol 18:52–74.

Dieu M, Vanbervliet B, Vicari A, Bridon J, Oldham E, Aït-Yahia S, Brière F, Zlotnik A, Lebecque S, Caux C. 1998. Selective recruitment of immature and mature dendritic cells by distinct chemokines expressed in different anatomic sites. J Exp Med 188:373–386.

Heresi G, Wang J, Taichman R, Chirinos J, Regalado J, Lichtstein D, Rosenblatt J. 2005. Expression of the chemokine receptor CCR7 in prostate cancer presenting with generalized lymphadenopathy: Report of a case, review of the literature, and analysis of chemokine receptor expression. Urol Oncol 23:261–267.

Hirakawa S, Brown L, Kodama S, Paavonen K, Alitalo K, Detmar M. 2007. VEGF-C-induced lymphangiogenesis in sentinel lymph nodes promotes tumor metastasis to distant sites. Blood 109:1010–1017.

Hirao M, Onai N, Hiroishi K, Watkins S, Matsushima K, Robbins P, Lotze M, Tahara H. 2000. CC chemokine receptor-7 on dendritic cells is induced after interaction with apoptotic tumor cells: Critical role in migration from the tumor site to draining lymph nodes. Cancer Res 60:2209–2217.

Issa A LT, Shoushtari AN, Shields JD, Swartz MA. 2009. Vascular endothelial growth factor-C and C-C chemokine receptor 7 in tumor cell-lymphatic cross-talk promote invasive phenotype. Cancer Res 69:349–357.

Karnoub A, Dash A, Vo A, Sullivan A, Brooks M, Bell G, Richardson A, Polyak K, Tubo R, Weinberg R. 2007. Mesenchymal stem cells within tumour stroma promote breast cancer metastasis. Nature 449:557–563.

Kido A, Yoshitani K, Shimizu T, Akahane M, Fujii H, Tsukamoto S, Kondo Y, Honoki K, Imano M, Tanaka Y. 2012. Effect of mesenchymal stem cells on hypoxia-induced desensitization of β2-adrenergic receptorsin rat osteosarcoma cells. Oncol Lett 4:745–750.

Kuhn NZ, Tuan RS. 2010. Regulation of stemness and stem cell niche of mesenchymal stem cells: Implications in tumorigenesis and metastasis. J Cell Physiol 222:268–277.

Li R, Younes M, Wheeler T, Scardino P, Ohori M, Frolov A, Ayala G. 2004. Expression of vascular endothelial growth factor receptor-3 (VEGFR-3) in human prostate. Prostate 58:193–199.

Liu FY ZZ, Li P, Ding X, Zong ZH, Sun CF. 2010. Mammalian target of rapamycin (mTOR) is involved in the survival of cells mediated by chemokine receptor 7 through PI3K/Akt in metastatic squamous cell carcinoma of the head and neck. Br J Oral Maxillofac Surg 48:291–296.

Ma M, Ye J, Deng R, Dee C, Chan G. 2011. Mesenchymal stromal cells may enhance metastasis of neuroblastoma via SDF-1/CXCR4 and SDF-1/CXCR7 signaling. Cancer Lett 312:1–10.

Mandriota S, Jussila L, Jeltsch M, Compagni A, Baetens D, Prevo R, Banerji S, Huarte J, Montesano R, Jackson D, Orci L, Alitalo K, Christofori G, Pepper M. 2001. Vascular endothelial growth factor-C-mediated lymphangiogenesis promotes tumour metastasis. EMBO J 20:672–682.

Murphy P, Baggiolini M, Charo I, Hébert C, Horuk R, Matsushima K, Miller L, Oppenheim J, Power C. 2000. International union of pharmacology. XXII. Nomenclature for chemokine receptors. Pharmacol Rev 52:145–176.

Olsson A, Dimberg A, Kreuger J, Claesson-Welsh L. 2006. VEGF receptor signalling—In control of vascular function. Nat Rev Mol Cell Biol 7:359–371.

Park SJ, Shin EJ, Min SS, An J, Li Z, Hee Chung Y, Hoon Jeong J, Bach JH, Nah SY, Kim WK, Jang CG, Kim YS, Nabeshima YI, Nabeshima T, Kim HC. 2013. Inactivation of JAK2/STAT3 signaling axis and downregulation of M1 mAChR cause cognitive impairment in klotho mutant mice, a genetic model of aging. Neuropsychopharmacology 38:1426–1437.doi: 10.1038/npp.2013.39

Rattigan Y, Hsu J, Mishra P, Glod J, Banerjee D. 2010. Interleukin 6 mediated recruitment of mesenchymal stem cells to the hypoxic tumor milieu. Exp Cell Res 316:3417–3424.

Sinha S VP, Bhattacharya R, Dutta S, Sinha S, Mukhopadhyay D. 2009. Dopamine regulates phosphorylation of VEGF receptor 2 by engaging Src-homology-2-domain-containing protein tyrosine phosphatase 2. J Cell Sci 122:3385–3392.

Sozzani S, Allavena P, D′Amico G, Luini W, Bianchi G, Kataura M, Imai T, Yoshie O, Bonecchi R, Mantovani A. 1998. Differential regulation of chemokine receptors during dendritic cell maturation: A model for their trafficking properties. J Immunol 161:1083–1086.

Veikkola T, Jussila L, Makinen T, Karpanen T, Jeltsch M, Petrova T, Kubo H, Thurston G, McDonald D, Achen M, Stacker S, Alitalo K. 2001. Signalling via vascular endothelial growth factor receptor-3 is sufficient for lymphangiogenesis in transgenic mice. EMBO J 20:1223–1231.

Zhong H, Semenza G, Simons J, De Marzo A. 2004. Up-regulation of hypoxia-inducible factor 1alpha is an early event in prostate carcinogenesis. Cancer Detect Prev 28:88–93.

Zlotnik A, Yoshie O. 2000. Chemokines: A new classification system and their role in immunity. Immunity 12:121–127.

SUPPORTING INFORMATION

Additional supporting information may be found in the online version of this article at the publisher′s web-site.